Tetrahedron 67 (2011) 1862–1872

Contents lists available at ScienceDirect

Tetrahedron

journal homepage: www.elsevier.com/locate/tet

Pyrrole azocrown ethers—synthesis, crystal structures, and fluorescence properties

Ewa Wagner-Wysiecka [a], Tomasz Rzymowski [a], Marina S. Fonari [b], Rafał Kulmaczewski [a], Elżbieta Luboch [a],*

[a] Gdansk University of Technology, Chemical Faculty, Department of Chemical Technology, 80-233 Gdańsk, Poland
[b] Institute of Applied Physics, Academy of Sciences, Chişinău MD 2028, Republic of Moldova

ARTICLE INFO

Article history:
Received 30 July 2010
Received in revised form 11 December 2010
Accepted 11 January 2011
Available online 15 January 2011

Keywords:
Crown ethers
Azo compounds
Pyrrole
Macrocyclisation
X-ray structure
Fluorescence spectroscopy
Lead(II) detection

ABSTRACT

Pyrrole containing macrocycles with chromophoric and fluorescent residues were prepared. X-ray structures for compounds **1** and **4** were determined. The presented pyrrole azocrowns are lead(II) chemosensors, which can be used both in UV–vis and fluorescence spectroscopy.

1. Introduction

The synthesis of macrocyclic compounds and investigation of their binding properties are research topics for several decades. Such systems are often used in analytical chemistry, clinical biochemistry and analysis, environmental protection etc.[1] Sensors are designed depending on the type of an analyte (metal cations, anions or neutral hosts) and the type of the samples in which the analyte will be detected.[2] One of the most important things is how the information of the chemical recognition is transduced to an analytically useful signal. In chromoionophores the chemical recognition is signaled by changes in color and absorption spectra upon analyte–ligand interaction. There are also known compounds, which can be used in rapid color tests for ionic species detection and/or determination.[3] The weak points of rapid colorimetric tests are the accuracy. Both UV–vis spectroscopy and so-called rapid tests are valuable tools because of their easy handling and low costs.

Thanks the high selectivity, sensitivity, response time, and the possibility of remote sensing (optical fibers), fluorescence measurements are good alternative for other analytical methods of metal cation detection.[4] In literature, many examples of fluorescent metal cation sensors are described.[4–10] Fluoroionophores are classified,[4] e.g., according to the nature of the photoinduced process (mainly photoinduced electron transfer, photoinduced charge transfer or excimer formation), that is, responsible for photophysical changes upon cation binding. Examples of fluoroionophores derived from a combination of a macrocyclic or acyclic residue with fluorophores, such as benzothiazole,[5,6] naphthalene,[7] binaphthyl,[8] or pyrene[9] are known. Warner et al. have recently published the review article where details, such as instrumentation, sample preparation, techniques of measurements, sensors, and applications of luminescence spectroscopy are described.[10]

Metal cations are selectively bound by a variety of chromophoric and fluorophoric macrocyclic ligands of different molecular shapes and sizes, modified with different donor atoms changing their affinity toward the respective ion. Due to relatively easy synthetic procedures, good optical and spectral properties, an azo group is often used as a chromophore. The chromophore unit may be located in a side arm of the ionophore molecule or may be an inherent part of the macrocycle.[11] Among such ionophores, crown ether type ligands constitute a considerable group of sensing materials.[11]

Previously, we have presented a series of differently sized macrocyclic chromoionophores where two azo groups and a heterocyclic residue were a part of the macrocycle.[12–14] Here we

---

* Corresponding author. Tel.: +48 58 347 1759; fax: +48 58 347 1949; e-mail address: elub@chem.pg.gda.pl (E. Luboch).

0040-4020/$ – see front matter © 2011 Elsevier Ltd. All rights reserved.
doi:10.1016/j.tet.2011.01.027

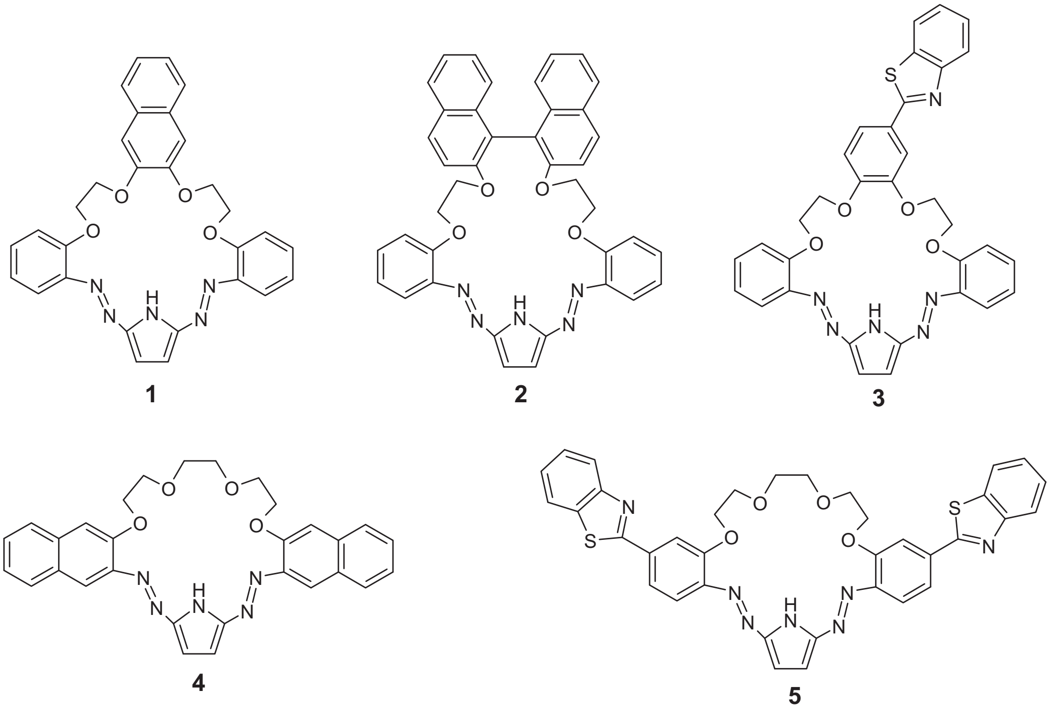

Fig. 1. Chemical structures of the macrocycles.

present the synthesis of a new group of crown ethers containing a heterocyclic—pyrrole residue (Fig. 1, compounds **2**–**5**). The new element of their structure is a fluorescent group introduced to a macrocycle skeleton. In compounds **1** (obtained earlier), **2**, and **3** the fluorophore is located in the polyether region of the molecule, whereas in ligands **4** and **5** it is a part of the chromophore's conjugated system. The crystal structures of ligands **1** and **4** were solved.

Cation metal complexation by the mentioned above chromogenic crown ethers was studied by means of UV–vis spectroscopy.[15] It was found that they preferentially bind lead(II) in acetonitrile and the stoichiometry of the formed complexes is solvent composition dependent. In pure acetonitrile a complex stoichiometry of 2:1 (L:M) was found, whereas in the solvent system containing a small amount of water (10%, v/v) 1:1 complex dominates. The highest value of the stability constant of lead complex in acetonitrile was obtained for compound **4** ($\log K_{L2Pb}$=12.2) and the lowest for **2** ($\log K_{L2Pb}$=9.0). For the comparison, the stability constant of lead(II) complex with **4** in mentioned above water containing system equals $\log K_{LPb}$=5.4.[15] It is worth attention, that both in acetonitrile, and its mixture with water, complexation is well pronounced in the absorption spectra with band separation about 100 nm between 'free' ligand and its complex. The observed spectral changes upon metal cation complexation are connected with color changes. As an example the color changes of ligand **5** solutions in the presence of the excess of the metal perchlorates, in acetonitrile, are shown in Fig. 2.

The fluorescence properties of the obtained compounds and its changes upon metal cation interaction are a part of the presented work.

2. Results and discussion

2.1. Synthesis

We synthesized macrocyclic compounds **2**–**5**, for which the presence of pyrrole ring substituted with two azo groups, polyether chain, and aromatic residues are the characteristic elements of their structure. The obtained compounds, besides **2**, which is 23-membered, are 21-membered macrocycles. In general, macrocyclic ligands **2**–**5** (Scheme 1) were obtained from diamino compounds (**7**, **9**, **11**, and **13**) by diazocoupling of the respective bisdiazonium salts with pyrrole under high dilution conditions and pH ~ 10. [14] Final products were purified by column chromatography. The compounds are reddish-brown (**2**–**4**) or violet (**5**) crystals with melting point over 200 °C. The detailed procedure of the synthesis of respective substrates and the final compounds (Scheme 1a–d) are given in experimental part. The synthetic route for crown **1** is described.[13] The investigations of the macrocycles presented here are a continuation of the studies on pyrrole bisazocrown ethers. By comparison with the previously described synthesis[13,14] some general conclusions could be drawn. The yield of the macrocyclisation is dependent on the structure of the aromatic amine. In a simple macrocyclisation,[14] 18- and 21-membered crowns were obtained with yields over 40%. In cases where the podand is bulky aromatic amine, steric effects may play a role in the diazocoupling reaction; the yield decreases dramatically even as low as 3% for azocrown **4** with two naphthalene residues.

2.2. X-ray crystallography

The structures of two azocrown ethers **1** and **4** were determined by X-ray diffraction analysis. Compounds **1**·H_2O and **4**·H_2O both

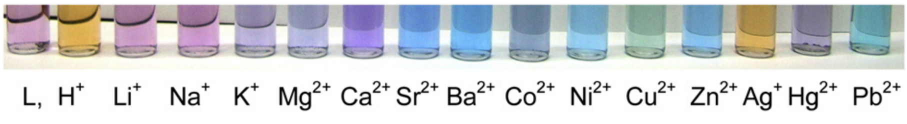

Fig. 2. The color changes of ligand **5** in the presence of the metal perchlorates excess (acetonitrile).

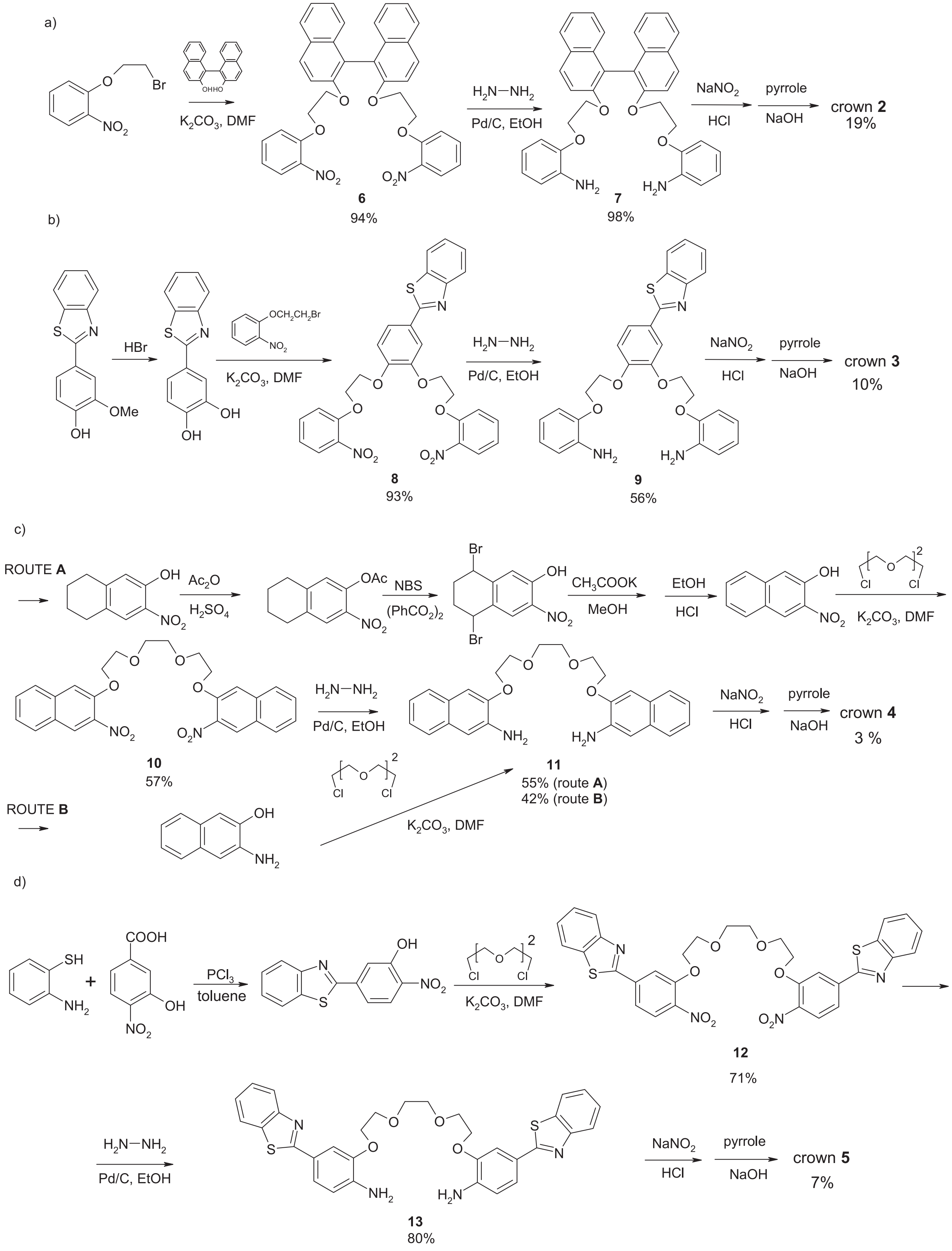

Scheme 1. The synthetic routes for crowns **2**–**5**.

crystallize in the monoclinic space group $P2_1/c$ with one hydrated macrocyclic molecule per asymmetric unit. The general view and atom numbering scheme for the molecules are shown in Fig. 3.

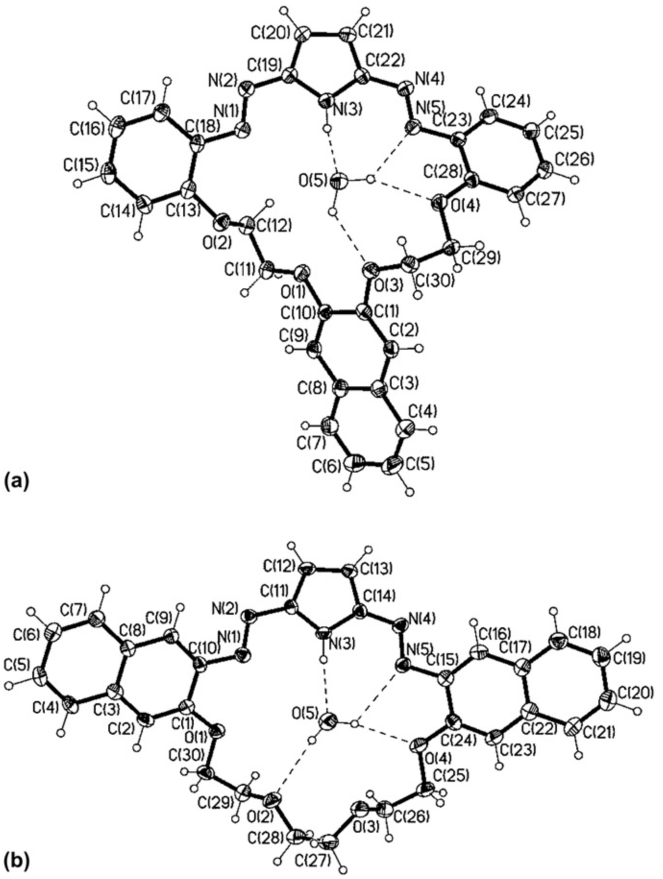

Fig. 3. ORTEP view of compounds **1**·H_2O (a) and **4**·H_2O (b) with atomic numbering scheme. Thermal ellipsoids are shown at the 50% probability level. Hydrogen bonds created by water molecule are shown by dashed lines.

The 21-membered macrocycle **1** consists of flexible dioxyethylene chains and four rigid aromatic moieties. The phenyl and pyrrole units are joined by two azo groups. Both azo groups in the molecule adopt the *E*-form with a *trans*-arrangement of carbo- and heterocyclic fragments (the same arrangement is registered in molecule **4**). The part of the macrocycle that incorporates phenyl and pyrrole rings and azo groups, represents a perfectly conjugated system with five nitrogen atoms lying approximately in the same plane with a mean deviation of ±0.041 Å. The conjugation is also obvious from the reduced values of the C–N bond distances [two of 1.376(3) and two of 1.417(3) Å, with the shortest distance till the phenyl carbon atom], and from the rough coplanarity of two phenyl and pyrrole rings. The dihedral angles phenyl(1) [C(13)–C(18)]/pyrrole [N(3), C(19)–C(22)]/phenyl(2) [C(23)–C(28)] are equal to 16.5(1) and 15.7(1)°, respectively. The geometry of this part of the macrocycle is close to that one in the recently reported methylimidazole analog[14] [where the dihedral angles phenyl(1)/imidazole/phenyl(2) are equal to 7.3, 13.0°, and 6.7, 5.3° in two independent molecules, respectively], and in the relative pyrrole thiacrown ether.[16]

In molecule **1** the phenyl rings attached to the macrocyclic framework display some bond length disturbance. Two of the three C–C bonds common to two rings (phenyl and crown ether) are elongated in this molecule; the C(1)–C(10) bond length is equal to 1.429(3) Å, the C(23)–C(28) bond length is equal to 1.408(3) Å, [C(13)–C(18) bond length equals to 1.398 Å, that corresponds to the standard value 1.399 Å]. The same peculiarity is characteristic of **4**. The corresponding bond lengths [C(1)–C(10) and C(15)–C(24)] in molecule **4** are also elongated to 1.442(4) and 1.429(5) Å, respectively. The authors[17] explain this phenomenon by the steric hindrance between the heteroatoms attached to the adjacent positions of the phenyl ring (in our cases O, O and N, O atoms in **1** and N, O atoms in **4**). The O(1)···O(3) distance between such oxygen atoms in **1** is equal to 2.518(2), which is shorter than twice the van der Waals radius (2.8 Å) of the oxygen atom, the N(1)···O(2) and N(5)···O(4) distances also reveal some shortening (the sum of the van der Waals radii of the N and O atoms is 3.0 Å), being 2.840(2) Å and 2.651(2) Å (bifurcated hydrogen bonding with water molecule also contributes to this shortening, see Fig. 3). Following to[17] we observe in **1** and **4** not only the elongation of the C–C bond but also the distortion of O–C(Ar)–C(Ar) and N–C(Ar)–C(Ar) bond angles, with the increased values for the external O(N)–C–C angles [122.7(2)–124.7(2)°] and reduced values for the internal angles [116.3(2)–118.5(2)°]. These distortions have been explained by the conjugation between the π-system of the phenyl ring and an oxygen atom lone electron pair (LEP). The bond angles at these oxygen atoms in **1** [117.1(2)–119.5(2)°] imply the sp^2 hybridization state being increased in comparison with the standard value (~112°) typical for the sp^3 hybridization.

Similar geometric peculiarities are observed in **4**. The N(1)···O(1) and N(5)···O(4) distances of 2.629 and 2.643 Å, respectively, are shorter than the sum of van der Waals radii for N and O (3.0 Å). The external bond angles O(1)–C(1)–C(2), N(1)–C(10)–C(9), C(16)–C(15)–N(5), and O(4)–C(24)–C(23) [125.9(3), 124.2(3), 124.7(3), and 124.6(3)°, respectively] all are essentially increased in comparison with the internal ones, O(1)–C(1)–C(10), N(1)–C(10)–C(1), N(5)–C(15)–C(24), and O(4)–C(24)–C(15) [114.4(3), 116.2(3), 116.3(3), and 115.1(3)°, respectively], bond angles at O(1) and O(4) atoms [117.1(3)° and 116.5(3)°] are greater than the bond angles at two other crown oxygen atoms [112.7(3)° and 113.3(3)°, respectively].

The attachment of a bulky naphthyl unit to the oxyethylene chain in **1** has a decisive influence on the conformation of this part of the molecule (Fig. 4) and results in its quite distorted shape with the naphthyl moiety being approximately equally inclined to both phenyl rings [the dihedral angles naphthyl/phenyl(1), naphthyl/phenyl (2) are equal to 51.3(1) and 62.4(1)°, respectively], and two oxygen atoms O(1) and O(4) being situated essentially lower and higher than the best plane of the molecule.

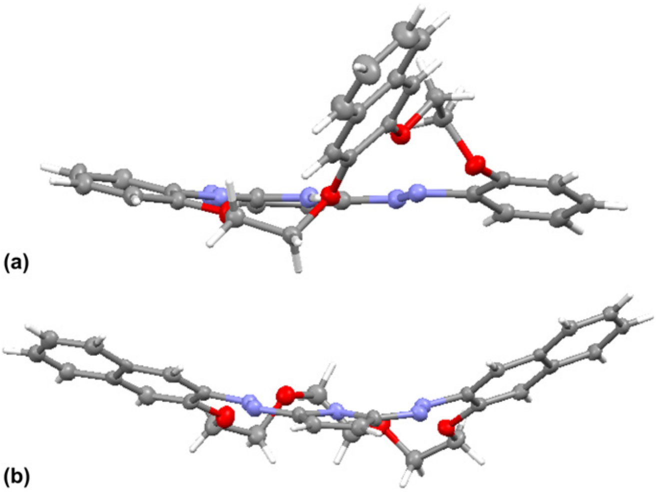

Fig. 4. Side view of macrocycles **1** (a) and **4** (b).

In the 21-membered macrocycle **4** three planar units, two naphthyl substituents [C(1)–C(10) atoms being coplanar within ±0.024 Å, C(15)–C(24) atoms being coplanar within ±0.037 Å], and pyrrole ring [N(3), C(11)–C(14) atoms being coplanar within ±0.005 Å] form the extended asymmetric conformation with the dihedral angles between the planes naphthyl(1)/pyrrole/naphthyl (2) units equal to 39.4(1) and 31.7(1)°, respectively (Fig. 4).

This butterfly-like arrangement of two bulky naphtho groups has been also registered in dinaphtho substituted crown ethers with the close ring size.[18] Because of the constraints imposed by the rigid segment of the molecule, the conjugated system comprising five nitrogen atoms acquires practically flat conformation with the atoms lying within ±0.025 Å of the mean plane, which they define. The geometry of this azo-part of the macrocyclic skeleton in **4** is in close concern with **1** and with the already cited macrocycles.[14,16] Four oxygen atoms of the oxyethylene chain are essentially displaced from this mean plane [the range is from +0.51 Å for O(3) up to +1.28 Å for O(2)], all in the same direction.

In the oxyethylene chain of **1** Csp^3–Csp^3 bonds are in a *gauche*-conformation, Csp^2–Csp^2 bonds are in a *cis*-conformation and of 8 C–O bonds, two adopt an energetically unfavorable *gauche*-conformation (Table 1); in comparison, only one C–O bond in **4** is in a *gauche*-conformation, thus the oxyethylene crown fragment in **4** reveals more ordered shape.

Table 1
Selected torsion angles [°] in **1** and **4**

1		**4**	
C(12)–O(2)–C(13)–C(18)	−63.2(2)	C(10)–C(1)–O(1)–C(30)	−178.8(3)
C(13)–O(2)–C(12)–C(11)	−159.1(2)	C(1)–O(1)–C(30)–C(29)	−174.0(3)
O(2)–C(12)–C(11)–O(1)	−70.6(2)	O(1)–C(30)–C(29)–O(2)	68.4(4)
C(12)–C(11)–O(1)–C(10)	179.6(2)	C(30)–C(29)–O(2)–C(28)	147.5(3)
C(11)–O(1)–C(10)–C(1)	172.8(2)	C(29)–O(2)–C(28)–C(27)	178.0(3)
O(1)–C(10)–C(1)–O(3)	0.7(3)	O(2)–C(28)–C(27)–O(3)	−65.0(4)
C(10)–C(1)–O(3)–C(30)	176.6(2)	C(28)–C(27)–O(3)–C(26)	−66.1(4)
C(1)–O(3)–C(30)–C(29)	91.1(2)	C(27)–O(3)–C(26)–C(25)	−155.2(3)
O(3)–C(30)–C(29)–O(4)	65.1(2)	O(3)–C(26)–C(25)–O(4)	−67.1(4)
C(30)–C(29)–O(4)–C(28)	175.3(2)	C(26)–C(25)–O(4)–C(24)	173.0(3)
C(29)–O(4)–C(28)–C(23)	175.6(12)	C(25)–O(4)–C(24)–C(15)	−177.0(3)

Both **1** and **4** neatly accommodate a water molecule, which is nesting at 0.65 Å from the mean plane of seven N_3O_4 heteroatoms. The water molecule is displayed practically in the center of the macrocycle and acts in an identical mode, as a hydrogen bond donor in one single and one bifurcated hydrogen bond, and as H-acceptor in N(3)–H···O(5) hydrogen bond toward pyrrole hydrogen. The hydrogen bonding geometry is listed in Table 2. This mode of water inclusion in the cavity is rather typical for macrocycles and podands that possess both H-acceptor and H-donor functionalities[19] (in **4** it practically reproduces methylimidazole analog).[12] The rearrangement of a single O(5)–H···O(crown) hydrogen bond in **1** in comparison with **4** is connected with incorporation of naphthyl moiety making O(1) atom inaccessible for participation in hydrogen bonding.

Table 2
Hydrogen bonding geometry in **1**·H_2O and **4**·H_2O [Å °]

D–H···A	d(D–H)	d(H···A)	d(D···A)	∠(DHA)	Symmetry transformation for acceptor
1·H_2O					
O(5)-H(5a)···O(4)	0.94(1)	2.20(2)	3.012(2)	144(2)	*x*, *y*, *z*
O(5)-H(5a)···N(5)	0.94(2)	2.20(2)	2.998(2)	142(2)	*x*, *y*, *z*
O(5)-H(5b)···O(1)	0.93(2)	2.29(1)	3.149(2)	155(2)	*x*, *y*, *z*
N(3)-H(3)···O(5)	0.88(1)	1.89(1)	2.766(2)	169(2)	*x*, *y*, *z*
4·H_2O					
O(5)-H(5a)···O(4)	0.95(2)	2.13(2)	3.030(3)	158(3)	*x*, *y*, *z*
O(5)-H(5a)···N(5)	0.95(2)	2.44(3)	3.088(4)	125(3)	*x*, *y*, *z*
O(5)-H(5b)···O(2)	0.90(2)	2.27(2)	3.119(4)	156(4)	*x*, *y*, *z*
N(3)-H(3)···O(5)	0.87(2)	2.10(2)	2.882(4)	150(3)	*x*, *y*, *z*
C(9)-H(9)···O(1)	0.95	2.51	3.409(4)	158	−*x*+1, *y*−1/2, −*z*+1/2
C(18)-H(18)···O(3)	0.95	2.57	3.404(5)	146	−*x*, −*y*, −*z*

Some features in the crystal packing of **4**·H_2O are worth mentioning. The complexes are combined into centrosymmetric dimers via CH···O hydrogen bonds (Table 2), and π–π stacking interactions between the overlapping naphthyl- and azo-units, the interplanar distance being 3.35 Å, and further stack along the *b* axis due to the interaction between the extended aromatic units (Fig. 5).

2.3. Metal cation complexation

As described earlier,[13,15] pyrrole chromogenic crown ethers selectively bind lead(II) cation. Introduction into the macrocycle skeleton, additionally to chromophore residue, fluorescent group (naphthalene, binaphthyl or phenylbenzothiazole residues) may provide to the more universal sensing materials, e.g., for UV–vis spectrophotometry and fluorimetry. Independently of this, pyrrole macrocycles work satisfactorily as ionophores in lead-selective electrodes.[13] We investigated changes in fluorescence spectra of the synthesized compounds in the presence of the excess of the metal perchlorates in acetonitrile. Characteristic bands of fluorescence spectra for crowns **1**–**5** are collected in Table 3. For all compounds emission bands (excited with the wavelength characteristic for the aromatic residues) were found in the UV region, only in case of the compound **5** emission spectrum shows band in the visible range.

It was found that the presence of alkali and alkaline earth metal salts causes noticeable, however not very large changes in fluorescence spectra. Relatively more significant fluorescence changes were observed in the presence of lead(II) salt. The observed lead(II) selectivity is in agreement with previous results obtained from UV–vis measurements. In the presence of nickel(II) and cobalt(II) salts, fluorescence spectra changed during the time scale of experiment and similar observations were made in UV–vis measurements. The changes in fluorescence spectra in the presence of metal salts are exemplified for ligands **1**, **3**, and **5** (Fig. 6).

The relative percent changes in fluorescence spectra (for emission bands given in Table 3) for compounds **1**–**5** in the presence of 100-fold excess of metal salts in acetonitrile are shown in Fig. 7.

In the case of **1**, for all investigated metal cations, the enhancement of fluorescence was observed with the highest changes for lead(II) perchlorate. Similarly for crown **3**, the fluorescence intensity was enhanced upon lead(II) binding, however this effect is smaller compared to ligand **1**.

For crowns **2**, **4**, and **5**, fluorescence quenching was observed upon lead complexation with the most noticeable decrease for compound **5**. The changes in fluorescence spectrum upon titration with lead(II)perchlorate for compound **5** are shown in Fig. 8b. Additionally, the changes in absorption spectrum in the presence of lead(II) salt (titration experiment) for the same compound are shown in Fig. 8a.

The different behavior of the studied compounds may be ascribed to structural factors.

Donor atoms participating in metal cation complex formation may be oxygens in the polyether chain and one of the nitrogen atom of the azo moiety(ies). In compounds **1** and **3** a fluorophore is bounded to a polyether linkage and isolated from the diazopyrrole part of the molecule. The additional aromatic ring influences the rigidity of the molecule and determinates the size of the macrocyclic cavity. The fluorophores in crowns **4** and **5**, are connected to a polyether linkage and azopyrrole residue, and are more distant and spaced from the oxygen coordination centers.

The effect of the alkali (A) and alkaline earth (B) metal cations presence on fluorescence intensity changes upon lead(II) complexation was also studied. The most interesting results were obtained for ligands **3** and **4** where almost no interference of the equimolar to lead(II) metal cations amounts on the fluorescence intensity was observed. The obtained results are shown in Fig. 9.

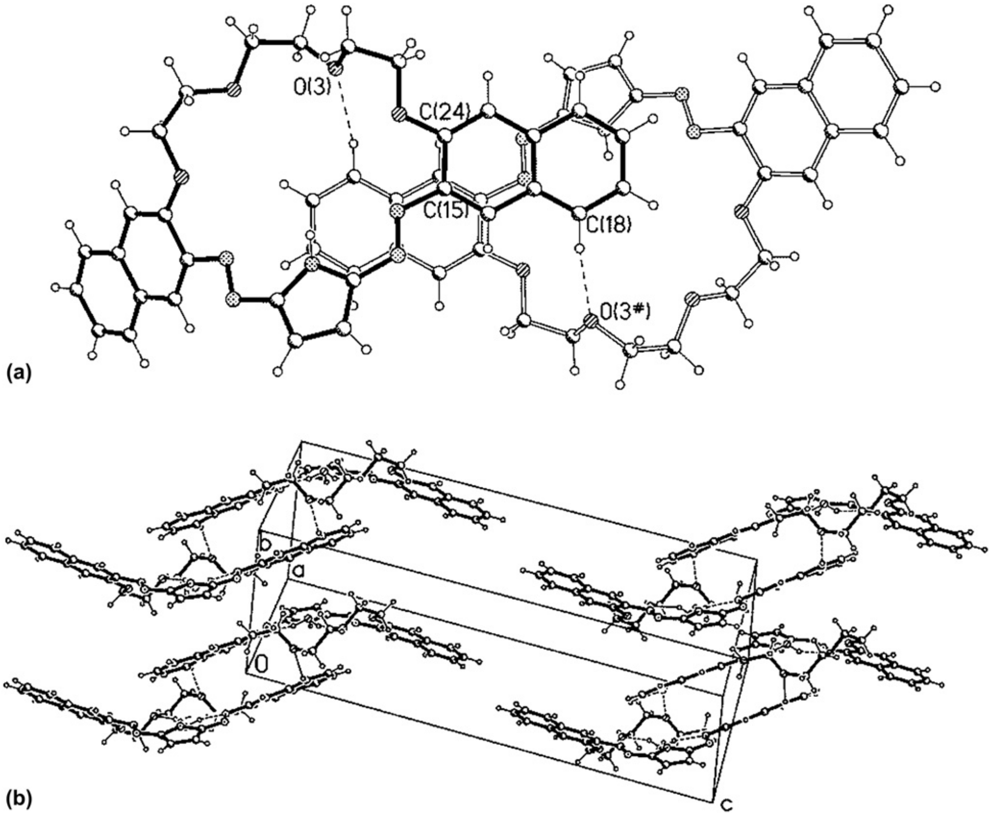

Fig. 5. (a) Top view of centrosymmetric dimers in **4**·H_2O. Labeled are the atoms participating in hydrogen bonding [C(18) and O(3)] and chosen to built the suitable projection. (b) stacking along *b* axis. Water molecules are omitted for clarity.

Table 3
Fluorescence measurements parameters for crowns **1**–**5**

Compound	λ_{ex}	λ_{em}
1	231	342
2	280	360
3	318	368, 386
4	300	393
5	316	420

3. Conclusions

A new class of pyrrole containing macrocycles with both chromophoric and fluorescent residues were prepared. The final procedure was diazocoupling of the respective bisdiazonium salt with pyrrole under high dilution conditions. It was found that the yield of the macrocyclisation is aromatic diamine structure dependent. The X-ray structure for compounds **1** and **4**, showing encapsulated a water molecule, was determined. It was found that these crowns are lead(II) chemosensors, which can be used not only in UV–vis but also in fluorescence spectroscopy. This means that compounds of this family are, to some extent, general for lead(II) selective sensing materials, which may be applied for different analytical tools.

4. Experimental

4.1. General

Unless otherwise stated, materials and solvents were of analytical reagent grade, and were obtained from the commercial suppliers and were used without further purification. For TLC experiments aluminum plates covered with Silica gel 60 F_{254} (Merck) were used. ^1H NMR spectra were recorded on Varian instrument at 500 MHz. Mass spectra were taken on AMD-604 and Mariner apparatus and IR spectra were recorded on Genesis II FTIR (Mattson) instrument. UV–vis measurements were carried with the use of UNICAM UV 300 Series spectrophotometer. Fluorescence spectra were acquired with the use of AMINCO Bowman, Series 2—luminescence spectrometer. Excitation and emission slits bandwidth: 8 nm. Both for UV–vis and fluorescence measurements 1 cm path length quartz cells were used. All measurements were carried out at room temperature.

4.2. General procedure for preparation of pyrrole azocrowns 2–5

Two solutions (A and B) were prepared:

(A) The respective diamine was stirred in water containing the appropriate amount of a mineral acid. To the ice cooled mixture, a solution of sodium nitrite was added. Diazotation reaction progress was controlled.
(B) Pyrrole and NaOH were dissolved in an ice cooled water with a small amount of alcohol.

The coupling reaction was carried out under high dilution technique by dropping solution A and B to the large volume of water alkalized with NaOH. The details are given below.

4.2.1. Azocrown ***1*** *was synthesized as described earlier.*[13]

4.2.2. Azocrown ***2****.* Compound was obtained from diamine **7** (0.26 g, 0.47 mmol) by diazotation with sodium nitrite (0.07 g in 1 mL of water) in the presence of HCl (0.24 mL concd HCl in 10 mL of water). Diazonium salt was coupled with pyrrole (0.035 mL, 0.5 mmol) dissolved in 10 mL of an ice cooled water containing 0.05 g NaOH and

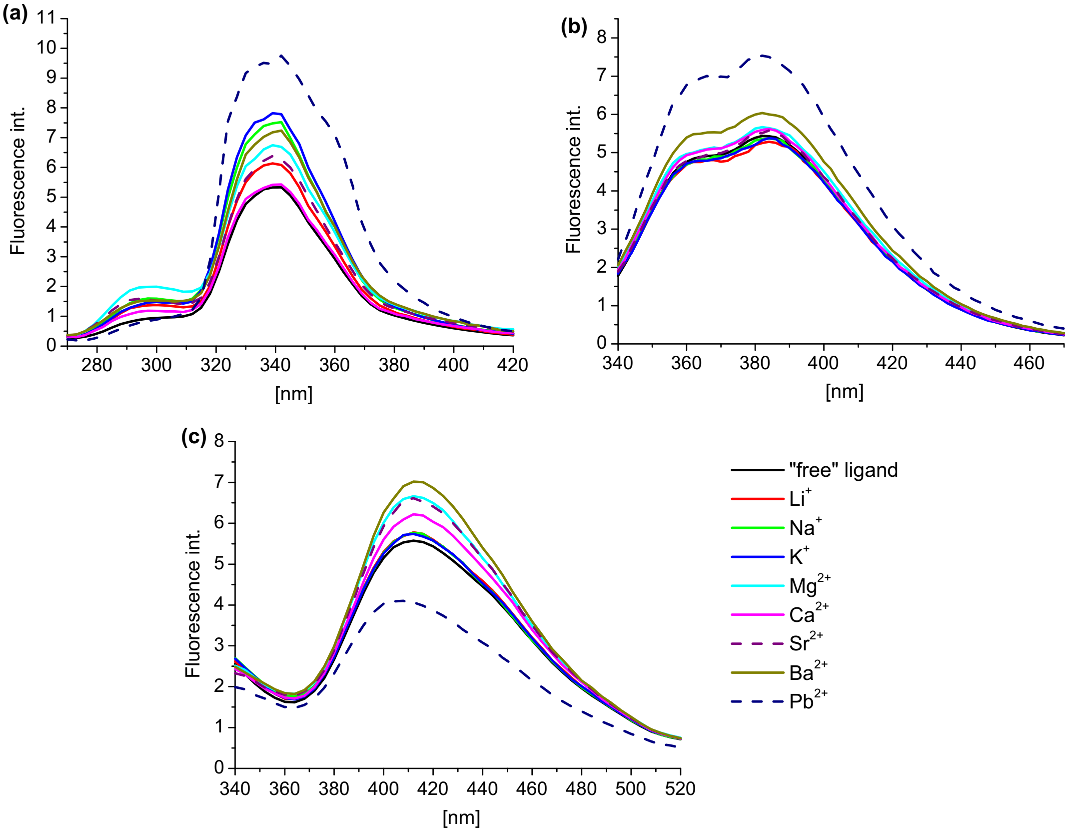

Fig. 6. The changes in fluorescence spectra in the presence of metal perchlorates (100-fold excess) for compounds (a) **1** (c=8.67×10^{-6} mol dm^{-3}); (b) **3** (c=9.30×10^{-6} mol dm^{-3}); (c) **5** (c=9.69×10^{-6} mol dm^{-3}).

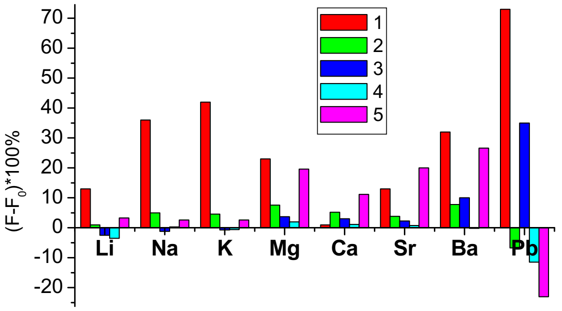

Fig. 7. The changes of fluorescence intensity for crowns **1**–**5** in the presence of 100-fold excess of metal perchlorates in acetonitrile. Changes in emission bands given in Table 3 were considered.

1 mL of ethanol. The two solutions were dropped simultaneously to a 150 mL of water (pH about 10 from NaOH). During 3 h, the stirred reaction mixture was kept at 10 °C and for the next 3 h at room temperature. The reaction progress was monitored by TLC. After that, to the reaction mixture acetic acid was added (to pH about 6) and solid was filtered off. Crown was isolated from the solid and purified with the use of column chromatography with the mixture of hexane–acetone (3:2) as an eluent. Yield 58 mg (19%) of brownish-red solid, mp 242–244 °C (from acetone–hexane). TLC (CH_2Cl_2–acetone, 30:1) R_f=0.93. ^{1}H NMR (acetone-d), δ [ppm]: 4.10–4.16 (2H, m); 4.28–4.34 (2H, m); 4.48–4.52 (4H, m); 6.95–7.20 (8H, m); 7.17 (2H, t, J=7.3 Hz); 7.21 (2H, s); 7.37 (2H, t, J=7.8 Hz); 7.63–7.67 (4H, m); 7.72 (2H, d, J=8.3 Hz); 7.82 (2H, d, J=9.3 Hz); ~10.7 (1H, s). IR (Nujol): 1620; 1586; 1504; 1485; 1270; 1262; 1235; 1158; 1085; 1025; 990; 930; 875; 805; 747; 683 cm^{-1}. UV–vis: λ_1=228 nm, ε_1=9.7×10^4; λ_2=292 nm, ε_2=1.6×10^4; λ_3=337 nm, ε_3=1.2×10^4; λ_4=377 nm, ε_4=1.1×10^4; λ_5=501 nm, ε_5=2.0×10^4. HRMS (ESI): [M+Na]$^+$=668.2240 calculated for $C_{40}H_{31}N_5O_4Na$ 668.22683.

4.2.3. Azocrown ***3***. Diamine **8** (0.33 g, 0.6 mmol) was dissolved in 11 mL of water containing 0.18 mL concd H_2SO_4 by warming the above mixture. Next, the mixture was cooled with ice and the solution of sodium nitrite (0.077 g in 4 mL of water) was added. Diazotation was carried out for 30 min.

Diazonium salt was coupled with pyrrole (0.045 mL, 0.6 mmol) dissolved in 15 mL of an ice cooled water containing 0.055 g NaOH and 1 mL of ethanol by adding them simultaneously dropwise to water (400 mL adjusted to pH about 12 by NaOH). During 3 h, the intensively stirred reaction mixture was kept at 0 °C and for next 18 h at room temperature. The reaction progress was monitored by TLC (CH_2Cl_2–acetone, 30:1). After that, acetic acid was added (to pH about 6) and solid was filtered off. Macrocycle **3** was isolated from the solid and purified with the use of column chromatography and a mixture of methylene chloride–acetone (30:1) as an eluent. Yield 38 mg (10%) of brownish-red solid, mp 209–212 °C. TLC (CH_2Cl_2–acetone, 30:1) R_f=0.51. ^{1}H NMR (acetone-d), δ [ppm]: 4.73–4.82 (8H, m); 7.10 (2H, t, J=7.6 Hz); 7.13–7.17 (2H, m); 7.29 (1H, d, J=8.5 Hz); 7.36 (1H, d, J=8.2 Hz); 7.42–7.46 (2H, m); 7.49–7.56 (3H, m); 7.68 (1H, d, J=8.2 Hz); 7.78 (2H, d, J=7.9 Hz); 7.89 (1H, d, J=1.5 Hz); 8.00 (1H, d, J=7.9 Hz); 8.05 (1H, d, J=7.9 Hz); 12.27 (1H, br s). IR (Nujol): 3431; 1586; 1519; 1267; 1234; 1157; 1058; 1031; 935; 751; 722 cm^{-1}. UV–vis: λ_1=217 nm, ε_1=3.2×10^4; λ_2=323 nm, ε_2=2.4×10^4; λ_3=374 nm, ε_3=9.0×10^3; λ_4=501 nm, ε_4=1.5×10^4. HRMS (EI): [M]$^+$=602.17039 calculated for $C_{33}H_{26}N_6O_4S$ 602.17366.

4.2.4. Azocrown ***4***. Diamine **11** (0.42 g, 1 mmol) was diazotized with sodium nitrite solution (0.14 g, 2 mmol in 1 mL of water) in the presence of hydrochloric acid (0.5 mL concd HCl in 20 mL of water).

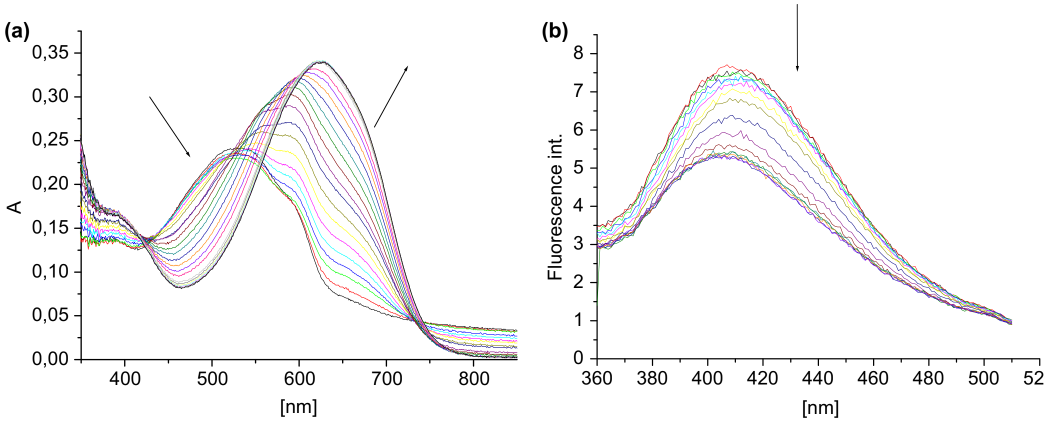

Fig. 8. (a) UV–vis titration of **5** (c_L=26.5×10^{-5} mol dm^{-3}) with lead(II) perchlorate (c_{Pb}=0–29×10^{-5} mol dm^{-3}); (b) fluorescence emission spectra of **5** upon titration (λ_{ex}=317; λ_{em}=420) (c_L=9.7×10^{-6} mol dm^{-3}) with lead(II) perchlorate (c_{Pb}=0–7.6×10^{-6} mol dm^{-3}) in acetonitrile.

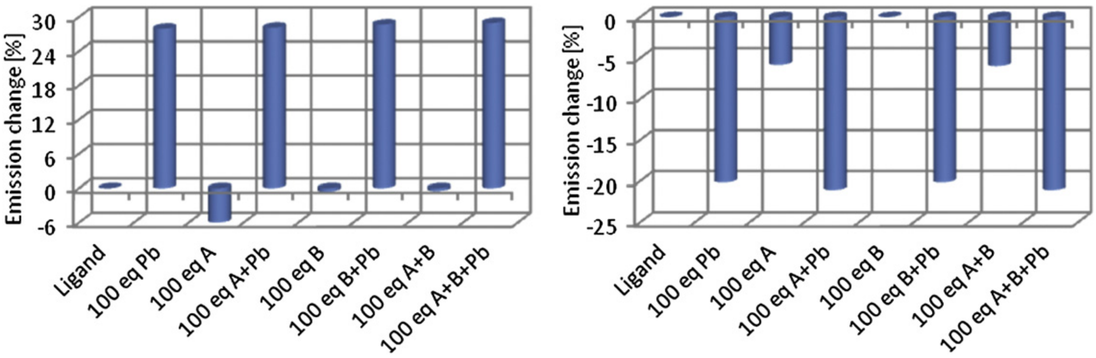

Fig. 9. The fluorescence intensity changes for crowns **3** (left) and **4** (right) in the presence of 100 equiv of lead(II) and equimolar amounts of alkali (A) and alkaline earth (B) metal cations in acetonitrile. Changes in emission bands given in Table 3 were considered.

The coupling reaction was carried out as follows: the diazonium salt and pyrrole (0.067 mL, 1 mmol) dissolved in an ice cooled water (20 mL) containing NaOH (0.01 g, 2.5 mmol) with the addition of ethanol (1 mL) were added dropwise to cool water (300 mL, pH 11 from NaOH). The mixture was allowed to stay at 10 °C for 3 h and for the next 3 h at room temperature. After it the mixture was cooled (5 °C) and acidified with acetic acid and solid filtered off. Product was isolated from the solid by column chromatography using a mixture of methylene chloride–acetone (30:1) as an eluent. Yield 16 mg (3%) of reddish-brown solid, mp 207–208 °C. TLC (methylene chloride–acetone, 30:1) R_f=0.73. ^{1}H NMR (acetone-*d*), δ [ppm]: 3.87 (4H, s); 3.98–4.05 (4H, m); 4.47–4.52 (4H, m); 7.32 (2H, s); 7.43 (2H, t, *J*=7.3 Hz); 7.53 (2H, t, *J*=7.8 Hz); 7.55 (2H, s); 7.86 (2H, d, *J*=8.2 Hz); 8.01 (2H, d, *J*=8.2 Hz); 8.04 (1H, s); 8.18 (1H, s); 13.21 (1H, br s). IR (film): 2924; 1621; 1594; 1448; 1360; 1249; 1180 cm^{-1}. UV–vis: λ_1=223 nm, ε_1=2.6×10^4; λ_2=346 nm, ε_2=3.0×10^3; λ_3=509 nm, ε_3=1.3×10^4. MS (EI): 521 calculated for $C_{30}H_{27}N_5O_4$ 521. HRMS (ESI): [M+Na]$^+$=544.1938 calculated for $C_{30}H_{27}N_5O_4Na$ 544.19553.

4.2.5. Azocrown ***5***. The diazonium salt was obtained from diaminopodand **13** (0.06 g, 0.11 mmol) dissolved in methanol (10 mL). To a clear solution concd HCl (0.07 mL) was added. To the ice cooled mixture, a solution of sodium nitrite (0.017 g in 1 mL of water) was added and kept at 0 °C for half an hour. Pyrrole (0.007 mL, 0.11 mmol) and NaOH (0.01 g) for coupling with diazonium salt were dissolved in an ice cooled mixture of water–methanol (1:10 v/v) and ice cooled. The solutions of diazonium salt and pyrrole were added dropwise to water–methanol mixture (500 mL, 1:1 v/v; pH about 11 from NaOH), the solution of the diazonium salt was added faster than the pyrrole solution. During 3 h, the intensively stirred reaction mixture was kept at 0 °C, and for the next 20 h at room temperature. After that, to the reaction mixture, acetic acid was added (to pH about 6), and solid was filtered off and washed with water. Macrocycle **5** was isolated from the solid using column chromatography with ethyl acetate–toluene (2:1) mixture as an eluent. Isolated product was rechromatographed in a mixture benzene–acetone (20:1) as an eluent giving 8 mg (7% yield) of crown ether (dark violet solid), mp 240 °C. TLC (ethyl acetate–toluene, 2:1) R_f=0.4. ^{1}H NMR (benzene-*d*), δ [ppm]: 3.22 (4H, s); 3.26–3.29 (4H, m); 3.69–3.73 (4H, m); 7.00 (2H, t, *J*=7.8 Hz); 7.06–7.20 (4H+solvent signal); 7.44 (2H, d, *J*=7.8 Hz); 7.57 (2H, d, *J*=8.3 Hz); 7.96 (2H, s); 7.99 (2H, d, *J*=8.3 Hz); 8.16 (2H, d, *J*=8.3 Hz); 14.00 (1H, s). IR (film): 3353; 1606; 1541; 1429; 1087; 1038; 876; 756 cm^{-1}. UV–vis: λ_1=218 nm, ε_1=1.2×10^4; λ_2=318 nm, ε_2=5.2×10^3; λ_3=378 nm, ε_3=4.2×10^3; λ_4=538 nm, ε_4=7.3×10^3. HRMS (EI): [M]$^+$=687.17062 calculated for $C_{36}H_{29}N_7O_4S_2$ 687.17225.

4.3. Synthesis of substrates 6–13

4.3.1. Compound ***6****. 2,2′-Bis[2-(2-nitrophenoxy)ethoxy]-1,1′-binaphthalene.* A mixture of 1,1′-binaphthalene-2,2′-diol (3.29 g, 11.5 mmol), 1-(2-bromoethoxy)-2-nitrobenzene (6.58 g, 26 mmol), K_2CO_3 (5.8 g), and dimethylformamide (30 mL) was stirred and heated at 80 °C for 20 h. The mixture was then diluted with water; the precipitate was separated, washed with water, dried, and next recrystallized from propan-2-ol. Yield 6.71 g (94%) of pale yellow solid, mp 165–167 °C. ^{1}H NMR ($CDCl_3$), δ [ppm]: 4.00–4.10 (4H, m); 4.24–4.36 (4H, m); 6.55 (2H, d, *J*=8.3 Hz); 6.92 (2H, t, *J*=7.8 Hz); 7.12 (2H, d, *J*=8.8 Hz); 7.15 (2H, t, J=7.3 Hz); 7.20 (2H, t, J=7.8 Hz); 7.34 (2H, t, J=7.2 Hz); 7.46 (2H, d, J=8.8 Hz); 7.71 (2H, d, J=7.8 Hz); 7.86 (2H, d, J=8.3 Hz); 7.95 (2H, d, J=9.3 Hz). IR (Nujol): 1604; 1589; 1519; 1327; 1234; 1166; 1145; 1092; 1041; 991; 972; 852; 807; 772; 744; 725 cm^{-1}. HRMS (EI): $[M]^+$=616.18357 calculated for $C_{36}H_{28}N_2O_8$ 616.18457.

4.3.2. Compound ***7****. 2,2′-Bis[2-(2-aminophenoxy)ethoxy]-1,1′-binaphthalene.* Hydrazine hydrate (98%, 2.5 mL) was dropped (3 h) to a suspension of dinitropodand **6** (3.08 g, 5 mmol) and Pd/C catalyst in boiling ethanol (100 mL). Heating was continued for 5 h. The hot mixture was filtered off and the solid residue was washed with hot ethanol. The filtrate was concentrated and allowed to stand whereupon the product crystallized. Yield 2.72 g (98%) of white solid, mp 115–116 °C. ^{1}H NMR (CDCl$_3$), δ [ppm]: 3.30 (4H, br s); 3.89–3.95 (4H, m); 4.29 (4H, t, J=4.6 Hz); 6.54 (2H, dd, J=8.3 and 1.5 Hz); 6.57–6.61 (4H, m); 6.76 (2H, dt, J=7.7 and 1.5 Hz); 7.14–7.20 (4H, m); 7.34–7.38 (2H, m); 7.50 (2H, d, J=9.3 Hz); 7.90 (2H, d, J=8.3 Hz); 7.98 (2H, d, J=9.3 Hz). IR (film): 3433; 3376; 3056; 2930; 2875; 1615; 1592; 1505; 1454; 1330; 1263; 1216; 1174; 1091; 1055; 986; 922; 809; 739 cm^{-1}. HRMS (EI): $[M]^+$=556.23536 calculated for $C_{36}H_{32}N_2O_4$ 556.23621.

4.3.3. Compound ***8****.* A mixture of 2-(3,4-dihydroxyphenyl)benzothiazole[3] (3.11 g; 12.8 mmol), 2-(2′-bromoethoxy)nitrobenzene (9.33 g, 4 mmol), and anhydrous potassium carbonate (5.3 g) in 60 mL of DMF was heated for 22 h at 75 °C. The reaction progress was monitored by TLC using a mixture of methylene chloride–acetone (30:1, v/v) as a mobile phase. The cooled reaction mixture was diluted with water. The crude solid product was filtered, washed with a mixture of water–methanol (1:1) and next with methanol. Yield 6.86 g (93%) of pale yellow solid, mp 119–120 °C. TLC (methylene chloride–methanol, 15:2) R_f=0.83. ^{1}H NMR (CDCl$_3$), δ [ppm]: 4.51 (4H, s); 4.55 (4H, s); 7.04 (2H, t, J=7.8 Hz); 7.10 (1H, d, J=8.3 Hz); 7.22 (2H, d, J=8.8 Hz); 7.39 (1H, t, J=7.6 Hz); 7.48–7.54 (3H, m); 7.67 (1H, dd, J=8.3 and 1.9 Hz); 7.80–7.83 (3H, m); 7.90 (1H, d, J=7.8 Hz); 8.06 (1H, d, J=8.3 Hz). IR (Nujol): 1608, 1583, 1522, 1352, 1281, 1269, 1258, 1196, 1134, 1037, 946, 853, 763, 739 cm^{-1}. HRMS (EI): $[M]^+$=573.12126 calculated for $C_{29}H_{23}N_3O_8S$ 573.12059.

4.3.4. Compound ***9****.* Compound **8** (3 g, 5 mmol) and Pd/C as catalyst were suspended in 120 mL of ethanol. To the boiling mixture, three portions (each of 1.1 mL) of hydrazine (98%) were added at 30 min intervals. Heating was continued for 20 h with reaction progress control by TLC (methylene chloride–acetone, 20:1). Catalyst was filtered off, washed with a hot mixture of ethanol–chloroform (1:1), then with chloroform, and then the collected filtrates were evaporated under reduced pressure. Pure product, white solid (1.5 g 56%) was obtained by crystallization from ethanol, mp 173–174 °C. TLC (methylene chloride–acetone, 20:1) R_f=0.60. ^{1}H NMR (DMSO-d_6), δ [ppm]: 4.29–4.32 (4H, m); 4.44–4.50 (4H, m); 4.71 (2H, s); 4.73 (2H, s); 6.51 (2H, dt, J=7.6 and 0.9 Hz); 6.61–6.63 (2H, m); 6.68–6.72 (2H, m); 6.88–6.92 (2H, m); 7.26 (1H, d, J=8.3 Hz); 7.44 (1H, dt, J=7.6 and 1.0 Hz) 7.54 (1H, dt, J=7.6 and 1 Hz); 7.66 (1H, dd, J=8.3 and 1.9 Hz); 7.79 (1H, d, J=1.9 Hz); 8.03 (1H, d, J=8.3 Hz); 8.12 (1H, d, J=7.3 Hz). IR (Nujol): 3452; 3358; 1609; 1499; 1263; 1219; 1131; 1059; 941; 737 cm^{-1}. HRMS (EI): $[M]^+$=513.17375 calculated for $C_{29}H_{27}N_3O_4S$ 513.17223.

4.3.5. Compound ***10****.* 3-Nitro-2-naphthol[20] (1.3 g, 6.6 mmol), 1,8-dichloro-3,6-dioxaoctane (0.5 mL, 3.3 mmol), and K_2CO_3 (1.4 g) in 2 mL of DMF was heated at 115 °C for 4 h. After water addition, the reaction mixture was extracted threefold with chloroform. Pure oily product was obtained with the use of column chromatography. As an eluent, methylene chloride (at the beginning) and then a mixture of methylene chloride–acetone (5:1) was used. Yield 0.9 g (57%) of yellow oil. TLC (methylene chloride–acetone, 50:1) R_f=0.55. ^{1}H NMR (CDCl$_3$), δ [ppm]: 3.74 (4H, s); 3.93 (4H, t, J=4.7 Hz); 4.40 (4H, t, J=4.7 Hz); 7.52 (2H, t, J=7.1 Hz); 7.64 (2H, t, J=7.3 Hz); 7.66 (2H, s); 7.90 (2H, d, J=8.2 Hz); 8.01 (2H, d, J=8.2 Hz); 8.40 (2H, s). IR (film): 3060; 2928; 2876; 1632; 1603; 1529; 1447; 1359; 1258; 1229; 1185; 1126; 1071; 953; 900; 869; 752; 476 cm^{-1}. HRMS (EI): $[M]^+$=492.15288 calculated for $C_{26}H_{24}N_2O_8$ 492.15327.

4.3.6. Compound ***11*** *(route A).* Dinitropodand **10** (0.87 g, 1.8 mmol) with a catalytic amount of Pd/C in ethanol (20 mL) was brought to boiling and then to the mixture, hydrazine (1 mL) in two portions (0.5 mL each) was added at 30 min intervals. Reaction was carried out for 4 h with progress control by TLC in methylene chloride–acetone (30:1) as a mobile phase. The catalyst was filtered off. Product crystallized from the cooled filtrate giving 0.43 g (55%) of bright yellow crystals, mp 88–90 °C. TLC (methylene chloride–acetone, 10:1) R_f=0.40. ^{1}H NMR (CDCl$_3$), δ [ppm]: 2.71 (4H, s); 3.81 (4H, s); 3.97 (4H, s); 4.30 (4H, t, J=4.6 Hz); 6.77 (2H, s); 7.07 (2H, s); 7.23 (2H, t, J=7.8 Hz); 7.28 (2H, s); 7.55 (2H, d, J=7.8 Hz); 7.60 (2H, d, J=6.8 Hz). IR (film): 3465; 3363; 3052; 2924; 2874; 1633; 1515; 1485; 1453; 1412; 1287; 1252; 1177; 1114; 945; 854; 745 cm^{-1}. HRMS (EI): $[M]^+$=432.20595 calculated for $C_{26}H_{28}N_2O_4$ 432.20491.

4.3.7. Compound ***11*** *(route B).* 3-Amino-2-naphthol (1.05 g, 6.6 mmol), 1,8-dichloro-3,6-dioxaoctane (0.5 mL, 3.3 mmol), and K_2CO_3 (1.4 g) in DMF (2 mL) were heated at 130 °C for 6 h. After water addition, crude product was precipitated. Pure product was obtained with the use of column chromatography with the mixture of methylene chloride–acetone (20:1) as an eluent. Yield 0.6 g (42%) of the same product as in the route A.

4.3.8. 2-(3-Hydroxy-4-nitrophenyl)benzothiazole. The synthesis was performed analogously to the synthesis of the isomeric compounds described in literature.[21]

To a solution of 3-hydroxy-4-nitrobenzoic acid (2.0 g, 11.0 mmol), 2-aminothiophenol (1.5 g, 11.0 mmol) in 20 mL of toluene, PCl_3 (0.9 mL, 10.0 mmol) was added dropwise at 45 °C. Heating at 112 °C was continued for 4 h. After 12 h at room temperature 20% Na_2CO_3 solution was added to the reaction mixture. Precipitate was filtered off and washed with water. The organic layer from the filtrate was evaporated under reduced pressure. To the remaining aqueous layer hydrochloric acid was added (to pH about 6) and the forming solid was filtered off. Three collected solids were crystallized from ethanol with a small addition of water giving the named product 2.23 g (72%), greenish-yellow solid, mp 212–214 °C. TLC (methylene chloride–acetone, 20:1) R_f=0.96. ^{1}H NMR (CDCl$_3$), δ [ppm]: 7.54 (1H, t, J=7.3 Hz); 7.60 (1H, t, J=7.3 Hz); 7.67 (1H, d, J=7.0 Hz); 7.87 (1H, s); 8.06 (1H, d, J=8.8 Hz); 8.14 (1H, d, J=8.8 Hz); 8.82 (1H, d, J=7.8 Hz); 11.50 (1H, s). IR (Nujol): 1621; 1582; 1503; 1313; 1260; 1155; 1069; 967; 895; 723; 655; 505 cm^{-1}. MS (EI): M^+=272; calculated for $C_{13}H_8N_2O_3S$ 272.

4.3.9. Compound ***12****.* 2-(3-Hydroxy-4-nitrophenyl)benzothiazole (**5**) (0.35 g, 1.2 mmol), K_2CO_3 (0.25 g, 1.76 mmol), 1,8-dichloro-3,6-dioxaoctane (0.1 mL, 0.66 mmol) in 5 mL of DMF were heated at 115 °C for 22 h. After cooling the reaction mixture was diluted with water and extracted with methylene chloride. The extract was dried with $MgSO_4$ and evaporated under reduced pressure. Product was isolated by column chromatography using a mixture of methylene chloride–acetone (50:1) as an eluent. Pure product, beige-yellow solid, 0.28 g (71%) was obtained by crystallization from mixture methylene chloride–hexane, mp 110–112 °C. TLC (methylene chloride–acetone, 50:1) R_f=0.22. ^{1}H NMR (CDCl$_3$), δ [ppm]: 3.82 (4H, s); 3.98 (4H, t, J=4.9 Hz); 4.44 (4H, t, J=4.9 Hz); 7.43 (2H, t, J=7.3 Hz); 7.55 (2H, t, J=7.3 Hz); 7.64 (2H, dd, J=8.3 and

1.5 Hz); 7.91–7.97 (6H, m); 8.12 (2H, d, *J*=8.3 Hz). IR (film): 2923; 2877; 1598; 1599; 1520; 1126; 1041; 926; 759 cm^{-1}. HRMS (EI): [M]$^+$=658.11620 calculated for $C_{32}H_{26}N_4O_8S_2$ 658.11921.

*4.3.10. Compound **13***. To dinitropodand **12** (0.32 g, 0.46 mmol) in 30 mL of mixture ethanol and water (1:1) ferric dust (0.278 g, 4.6 mmol) was added. To a boiling mixture acetic acid (0.14 mL) was added and refluxing was continued for 17 h. After that, the mixture was extracted with methylene chloride. The extract was concentrated and chromatographed on column using a mixture of methylene chloride and acetone (10:1), to give 0.23 g (80%) of an oily product. TLC (methylene chloride–acetone, 10:1) R_f=0.20. ^{1}H NMR ($CDCl_3$), δ [ppm]: 3.77 (4H, s); 3.91 (4H, t, *J*=4.4 Hz); 4.31 (4H, t, *J*=4.4 Hz); 4.4 (4H, br s); 6.72 (2H, d, *J*=8.3 Hz); 7.32 (2H, t, *J*=7.6 Hz); 7.45 (2H, t, *J*=7.6 Hz); 7.48 (2H, dd, *J*=7.8 and 1.4 Hz); 7.68 (2H, s); 7.84 (2H, d, *J*=7.8 Hz); 8.00 (2H, d, *J*=7.8 Hz). IR (film): 3461; 3350; 1617; 1303; 1247; 1140; 933; 876; 752 cm^{-1}. HRMS (EI): [M]$^+$=598.16968 calculated for $C_{32}H_{30}N_4O_4S_2$ 598.17085.

4.4. X-ray crystallographic studies

Crystals of **1**·H_2O and **4**·H_2O suitable for X-ray crystallography were grown by slow evaporation from acetone solutions. X-ray measurements for **1**·H_2O and **4**·H_2O were carried out on a KUMA KM4 four-axis diffractometer equipped with a Sapphire-2 CCD detector (Oxford Diffraction). The monocrystal was thermostated at 120 K in a nitrogen flow (Oxford Cryosystem). Data collection: CrysAlis CCD (Oxford Diffraction, 2005); cell refinement: CrysAlis RED (Oxford Diffraction, 2005);[22] data reduction: CrysAlis RED; program used to solve structure: SHELXS97; program used to refine structure: SHELXL97.[23] No absorption corrections were applied because of negligible influence of absorption on intensity of reflections (low μ values). All non-hydrogen atoms were refined anisotropically. *C*-bound hydrogen atoms were refined in geometrically idealized positions with isotropic temperature factors 1.2 times the equivalent isotropic temperature factors U equiv of their attached atoms. N- and O-bound hydrogen atoms were localized on difference Fourier map and refined in isotropic approximation.

Crystal/refinement data for **1**·H_2O: $C_{30}H_{27}N_5O_5$, M=537.57, monoclinic, space group $P2_1/c$, a=10.6091(6), b=10.5637(8), c=23.9467(13) Å, β=98.653(4)°, V=2653.2(3) Å^3, Z=4, T=120(2) K, D_c=1.346 g cm^{-3}, μ (Mo Kα)=0.094 mm^{-1}, F(000) 1128, 5182 unique reflections to 2θmax=52.0°, 370 refined parameters, GOF 1.020, R_1=0.0530, wR_2=0.0945 for 3150 observations with $I>2\sigma(I)$, R_1=0.1091, wR_2=0.1077 (for all unique data), largest diff. peak and hole: 0.232 and −0.203 e/Å^3.

Crystal/refinement data for **4**·H_2O: $C_{30}H_{29}N_5O_5$, M=539.58, monoclinic, space group $P2_1/c$, a=10.269(1), b=9.551(1), c=26.977(2) Å, β=96.87(1)°, V=2626.9(4) Å^3, Z=4, T=120(2) K, D_c=1.364 g cm^{-3}, μ (Mo Kα)=0.095 mm^{-1}, F(000) 1136, 4634 unique reflections to 2θmax=50.30°, 370 refined parameters, GOF 0.988, R_1=0.0714 for 2222 observations with $I>2\sigma(I)$, R_1=0.1770, wR_2=0.1158 (for all unique data), largest diff. peak and hole: 0.265 and −0.301 e/Å^3.

CCDC 646845 (**1**·H_2O) and CCDC 646846 (**4**·H_2O) contain the supplementary crystallographic data for this paper. These data may be obtained free of charge from The Cambridge Crystallographic Data Centre via www.ccdc.cam.ac.uk/data_request/cif.

4.5. Fluorescence measurements

Stock solution of all reagents (about 10^{-4} mol dm^{-3} for ligands and about 10^{-3} mol dm^{-3} for metal perchlorates) were prepared by weighing the appropriate amount of each compound and dissolving it in an acetonitrile. To prepare working solutions, an aliquot of a stock solution was placed in a 10 mL flask and diluted with the solvent. To the ligand solution, 100-fold excess of the metal salt solution was added and the fluorescence spectrum was registered. Measurements were repeated three times and the obtained results were averaged.

Acknowledgements

M.S.F. thanks the Foundation for Polish Science (FNP) and Mianowski Fund for received grant. The authors kindly acknowledged support from sources for science in years 2008–2010, Grant No. N N204 223834. Authors thank Jarosław Chojnacki Ph.D., D.Sc. for X-ray measurements.

Supplementary data

Supplementary data associated with this article can be found in the online version at doi:10.1016/j.tet.2011.01.027.

References and notes

1. *Comprehensive Supramolecular Chemistry*; Gokel, G. W., Ed.; Pergamon: New York, NY, 1996; Vol. 1.
2. *Macrocyclic Chemistry, Current Trends and Future Perspectives*; Gloe, K., Ed.; Springer: Dordrecht, The Netherlands, 2005.
3. Sheng, R.; Wang, P.; Gao, Y.; Wu, Y.; Liu, W.; Ma, J.; Li, H.; Wu, S. *Org. Lett.* **2008**, *10*, 5015–5018.
4. Valeur, B.; Leray, I. *Coord. Chem. Rev.* **2000**, *205*, 3–40.
5. Mashraqui, S. H.; Kumar, S.; Vashi, D. *J. Inclusion Phenom. Macrocyclic Chem.* **2004**, *48*, 125–130.
6. Kapor, S.; Sapre, A. V.; Kumar, S.; Mashraqui, S. H.; Mukherjee, T. *Chem. Phys. Lett.* **2005**, *408*, 290–294.
7. Hama, H.; Morozumi, T.; Nakamura, H. *Tetrahedron Lett.* **2007**, *48*, 1859–1861.
8. Wang, Y.-W.; Shi, Y.-T.; Peng, Y.; Zhang, A.-J.; Ma, T.-H.; Dou, W.; Zhang, J.-R. *Spectrochim. Acta, Part A* **2009**, *72*, 322–326.
9. Xie, J.; Ménand, M.; Maisonneuve, S.; Métivier, R. *J. Org. Chem.* **2007**, *72*, 5980–5985.
10. Powe, A. M.; Das, S.; Lowry, M.; El-Zahab, B.; Fakayode, S. O.; Geng, M. L.; Baker, G. A.; Wang, L.; McCarroll, M. E.; Patonay, G.; Aljarrah, M.; Li, M.; Neal, S.; Warner, I. M. *Anal. Chem.* **2010**, *82*, 4865–4894.
11. Luboch, E.; Bilewicz, R.; Kowalczyk, M.; Wagner-Wysiecka, E.; Biernat, J. F. *Advances in Supramolecular Chemistry: Azo Macrocyclic Compounds*; Cerberus: South Miami USA, 2003; Vol. 9, pp 73–163.
12. Wagner-Wysiecka, E.; Luboch, E.; Kowalczyk, M.; Biernat, J. F. *Tetrahedron* **2003**, *59*, 4415–4420.
13. Luboch, E.; Wagner-Wysiecka, E.; Fainerman-Melnikova, M.; Lindoy, L. F.; Biernat, J. F. *Supramol. Chem.* **2006**, *18*, 593–601.
14. Wagner-Wysiecka, E.; Jamrógiewicz, M.; Fonari, M. S.; Biernat, J. F. *Tetrahedron* **2007**, *63*, 4414–4421.
15. Wagner-Wysiecka, E.; Rzymowski, T.; Luboch, E. *Pol. J. Chem.* **2008**, *82*, 1299–1302.
16. Szczygelska-Tao, J.; Fonari, M. S.; Biernat, J. F. *Supramol. Chem.* **2008**, *20*, 651–658.
17. (a) Gromov, S. P.; Dmitrieva, S. N.; Vedernikov, A. I.; Kuz'mina, L. G.; Churakov, A. V.; Strelenko, Y. A.; Howard, J. A. K. *Eur. J. Org. Chem.* **2003**, 3189–3199; (b) Fedorova, O. A.; Fedorov, Y. V.; Vedernikov, A. I.; Yescheulova, O. V.; Gromov, S. P.; Alfimov, M. V.; Kuz'mina, L. G.; Churakov, A. V.; Howard, J. A. K.; Zaitsev, S. Y.; Sergeeva, T. I.; Möbius, D. *New J. Chem.* **2002**, *26*, 543–553.
18. (a) Panneerselvam, K.; Chacko, K. K.; Weber, E.; Kohler, H.-J. *J. Inclusion Phenom. Mol. Recognit. Chem.* **1990**, *9*, 337–347; (b) Weber, E.; Kohler, H.-J.; Reuter, H. *Chem. Ber.* **1989**, *122*, 959–967; (c) Panneerselvam, K.; Sobhia, M. E.; Chacko, K. K.; Weber, E.; Kohler, H.-J.; Pollex, R. *J. Inclusion Phenom. Mol. Recognit. Chem.* **1992**, *13*, 29–36; (d) Reddy, P. J.; Chacko, K. K.; Weber, E.; Kohler, H.-J.; Pollex, R. *Supramol. Chem.* **1993**, *3*, 47–56.
19. For examples of crown ethers encapsulating water molecule see (a) Huszthy, P.; Vermes, B.; Bathori, N.; Czugler, M. *Tetrahedron* **2003**, *59*, 9371–9377; (b) Suh, I.-H.; Namgung, H.; Ku Yoon, Y.; Saenger, W.; Vogtle, F. *J. Inclusion Phenom. Mol. Recognit. Chem.* **1985**, *3*, 21–26; (c) Bocskei, Z.; Simon, K.; Nemeth, V.; Agai, B.; Toke, L. *Acta Crystallogr.* **1996**, *B52*, 194–200; (d) Declercq, J.-P.; Tinant, B.; Dutasta, J.-P.; Mulatier, J.-C. *Phosphorus, Sulfur Silicon Relat. Elem.* **1999**, *155*, 1–14; (e) Huang, F.; Slebodnick, C.; Switek, K. A.; Gibson, H. W. *Chem. Commun.* **2006**, 1929–1932; (f) Luboch, E.; Wagner-Wysiecka, E.; Poleska-Muchlado, Z.; Kravtsov, V. C. *Tetrahedron* **2005**, *61*, 10738–10747; (g) Kraft, D.; Cacciapaglia, R.; Bohmer, V.; El-Fadl, A. A.; Harkema, S.; Mandolini, L.; Reinhoudt, D. N.; Verboom, W.; Vogt, W. *J. Org. Chem.* **1992**, *57*, 826–834; (h) Hiratani, K.; Goto, M.; Nagawa, Y.; Kasuga, K.; Fujiwara, K. *Chem. Lett.* **2000**, 1364–1366; (i) Palmer, R. A.; Potter, B. S.; Lisgarten, J. N.; Fenn, R. H.; Mason, S. A.; Mills, O. S.; Robinson,

P. M.; Watt, C. I. F. *Acta Crystallogr.* **2001**, *B57*, 339–345; (j) Dutasta, J.-P.; Declercq, J.-P.; Esteban-Calderon, C.; Tinant, B. *J. Am. Chem. Soc.* **1989**, *111*, 7136–7144; (k) Vichet, A.; Galy, J. P.; Baldy, A.; Barbe, J.; Feneau-Dupont, J.; Declercq, J.-P. *Acta Crystallogr.* **1991**, *C47*, 2508–2510; (l) Martinez, A.; Hemmert, C.; Gornitzka, H.; Meunier, B. *J. Organomet. Chem.* **2005**, *690*, 2163–2171.

20. Woodcock, W.; Clifford, D. R. *J. Chem. Soc.* **1957**, 4139–4141.
21. Anthony, K.; Brown, R. G.; Hepworth, J. D.; Hodgson, K. W.; May, B. *J. Chem. Soc., Perkin Trans. 2* **1984**, 2111–2117.
22. Oxford Diffraction. *CrysAlis CCD and CrysAlis RED*; Oxford Diffraction Poland: Wrocław, Poland, 2001.
23. Sheldrick, G. M. *SHELXS97 & SHELXL97. Programs for the Solution and Refinement of Crystal Structures*; University of Göttingen: Germany, 1997.